THE JOURNAL OF BIOLOGICAL CHEMISTRY
Vol. 277, No. 12, Issue of March 22, pp. 10474–10481, 2002
Printed in U.S.A.

rab4 Regulates Transport to the Apical Plasma Membrane in Madin-Darby Canine Kidney Cells*

Received for publication, November 26, 2001
Published, JBC Papers in Press, January 14, 2002, DOI 10.1074/jbc.M111237200

Karin Mohrmann, Richtje Leijendekker, Lisya Gerez, and Peter van der Sluijs‡

From the Department of Cell Biology, University Medical Center Utrecht and Institute of Biomembranes, 3584 CX Utrecht, The Netherlands

The small GTPase rab4 is associated with early endosomes and regulates membrane recycling in fibroblasts. rab4 is present in epithelial cells; however, neither its localization nor function has been established in this cell type. We transfected Madin-Darby canine kidney cells with rab4, the GTPase-deficient mutant rab4Q67L, and the dominant negative mutant rab4S22N that poorly binds guanine nucleotides. Confocal immunofluorescence microscopy showed that rab4 was concentrated on internal structures at the lateral side of the cell around the nucleus. Quantitative immunoelectron microscopy revealed that the majority of rab4 was localized in the upper third of the cytoplasm. In cell surface binding experiments with ^{125}I-transferrin, we found a redistribution of transferrin receptor from the basolateral to the apical plasma membrane in cells expressing rab4 and rab4Q67L. After accumulation of transferrin at 16 °C in basolateral early endosomes, rab4 and rab4Q67L increased the amount of apically targeted transferrin receptor. A qualitatively similar effect was obtained in control cells treated with brefeldin A. The effects of brefeldin A and rab4 on apical targeting of transferrin receptor were not additive, suggesting that brefeldin A and rab4 may act in the same transport pathway from common endosomes.

Eukaryotic cells internalize cell surface proteins and material from their environment by endocytosis. The pathway is used for the uptake of nutrients, regulation of cell surface receptors, and recycling of proteins used in the secretory pathway. Ligands are bound to receptors at the plasma membrane. The complex then enters clathrin-coated pits, is internalized in clathrin-coated vesicles, and transported to early endosomes (EEs),[1] where sorting occurs to different compartments. The mildly acidic pH in EEs causes dissociation of several ligand-receptor complexes. Ligands are then targeted to late endosomes/lysosomes for degradation, whereas most receptors are transported via recycling endosomes back to the cell surface for reutilization (reviewed in Ref. 1). Although receptor recycling is relatively well understood at the phenomenological level, little is known about the molecular principles that regulate vesicular transport from EEs to recycling endosomes and the plasma membrane.

An additional layer of complexity in the regulation of endocytic pathways is present in polarized epithelial cells. These have biochemically distinct apical and basolateral plasma membrane domains that are separated by tight junctions. Endocytosis occurs at both poles of this cell type. Earlier studies in Madin-Darby canine kidney (MDCK) cells suggested that apically and basolaterally internalized fluid phase tracers enter distinct apical and basolateral EEs before they reach a common late endosomal compartment (2). However, more recent investigations with ligands of transcytosing and recycling receptors revealed that basolateral and apical EEs are also interconnected (3–6) and converge to the common early endosome (CE). The CE is an extensively tubularized organelle that is accessible to basolaterally internalized and recycled transferrin receptor (TfR) but also to basolaterally endocytosed polymeric IgA receptor (pIgAR) before it reaches the apical plasma membrane (7). Fluid phase tracers enter the CE at relatively low concentrations because these have already been sorted in the basolateral or apical EEs. Recycling receptors such as TfR and the transcytosing pIgAR are most likely sorted in the CE. pIgAR is subsequently transported to the apical recycling endosome (ARE) before it reaches the apical cell surface. The ARE is typically devoid of Tf, which is transported from the CE to the cell surface and possibly apical EEs (see Ref. 8). Although little is known about the biochemical composition of the ARE, it is enriched in proteins and lipids typically found in rafts (9), whereas the lumenal pH of 6.3–6.5 is considerably less acidic that that of basolateral and apical EEs (6, 9). Because sorting of TfR occurs in both EEs and the CE, it is not clear whether transit through the CE is a prerequisite for basolaterally recycling receptors (4, 10).

Testifying to the high degree of complexity of endosomal pathways is the increasing number of small GTPases that have been localized to the cytosolic surface of early endocytic organelles. For instance, rab5 is associated with basolateral and apical EEs (11), whereas its effector EEA1 is predominantly associated with basolateral EEs (12), suggesting that the spatiotemporal regulation of rab5 activity may be different at these two early endosome populations. Testifying to this notion is the recent discovery that the rab5 effector Vps34p differentially regulates endocytosis at the apical and basolateral surface in WIF-B cells (13). We have been investigating the role of rab4 in transport through the early endocytic pathway (14, 15). rab4 is localized to early endocytic compartments and transport vesicles but not to the plasma membrane (16, 17) and regulates recycling of cell surface receptors (14, 18). How rab4

* This work was supported by grants from the Netherlands Organization for Medical Research and the Dutch Cancer Society (to P. v. d. S.). The costs of publication of this article were defrayed in part by the payment of page charges. This article must therefore be hereby marked "*advertisement*" in accordance with 18 U.S.C. Section 1734 solely to indicate this fact.

‡ To whom correspondence should be addressed: Dept. of Cell Biology, Utrecht University School of Medicine, AZU Rm. G02.525, Heidelberglaan 100, 3584 CX Utrecht, The Netherlands. Tel.: 31-302507574; Fax: 31-302541797; E-mail: pvander@knoware.nl.

[1] The abbreviations used are: EE, early endosome; ARE, apical recycling endosome; BFA, brefeldin A; BSA, bovine serum albumin; CE, common early endosome; EEA1, early endosome-associated antigen 1; MDCK, Madin-Darby canine kidney; pIgAR, polymeric IgA receptor; Tf, transferrin, TfR, transferrin receptor; dIgA, dimeric IgA; MEM, minimum Eagle's medium; PBS, phosphate-buffered saline; gp80, glycoprotein 80; ARF, ADP ribosylation factor 1; CHO, Chinese hamster ovary.

mediates its function is not yet clear, but the cloning and functional characterization of bifunctional effector proteins such as the rabaptins suggest that the sequential and opposite activities of rab5 and rab4 on EE membrane dynamics are coordinated through these effector proteins. Here we generated stable MDCK transfectants ectopically expressing wild type and mutant rab4. Our results show that rab4 controls transport of TfR from the CE to the apical plasma membrane.

MATERIALS AND METHODS

Antibodies and Expression Constructs—Rabbit antibodies against rab4 and mouse monoclonal antibodies 9E10 and NH against the myc and influenza X31 NH epitope tags have been described previously (15, 19, 20). The rat monoclonal antibody against ZO-1 and rabbit antibodies against gp80 and EEA-1 were generously provided by Karl Matter (University of Geneva), Claudia Koch-Brandt (Johannes Gutenberg University, Mainz, Germany), and Michael Clague (University of Liverpool), respectively. Dimeric IgA (dIgA) was generously provided by by Jean-Pierre Vaerman (Catholic University of Louvain, Louvain, Belgium). Rabbit antibodies against rab11 and IgA were purchased from Zymed Laboratories Inc. and DAKO, respectively rabbit. Fluorescence-labeled secondary antibodies were from Molecular Probes (Leiden, The Netherlands) and Jackson ImmunoResearch Laboratories (Westgrove, PA). myc-tagged human TfR cDNA was excised with *Sac*I and *Xba*I from mycTfR-pCB6 (21) and ligated in pCB7 (generously provided by Jim Casanova; Harvard University). rab4, rab4S22N, and rab4Q67L were released with *Eco*RI from corresponding pGBT9 constructs (22) and cloned in the same site of pcDNA3 (Invitrogen). NH-tagged rab4 constructs were as described previously (23).

Cell Culture and Transfection—MDCKII cells were grown in MEM (Invitrogen) and 10% fetal calf serum supplemented with 100 units/ml penicillin and 100 μg/ml streptomycin. The cells were transfected with mycTfR-pCB7 as described previously (23), and transfectants were selected in media containing 200 units/ml hygromycin. Expression was screened by immunofluorescence microscopy after 2 weeks. Positive clones were assayed for their ability to internalize and recycle ^{125}I-Tf and subcloned by limited dilution. A representative clone with TfR kinetics identical to those of endogenous canine TfR (24) was transfected with rab4, rab4S22N, and rab4Q67L in pcDNA3. Double transfectants were selected in media containing 200 units/ml hygromycin and 0.6 mg/ml G418. Colonies were screened after 2 weeks by immunofluorescence microscopy, subcloned by limited dilution cloning, and re-evaluated by immunofluorescence microscopy, Western blot, and ^{125}I-Tf single cycle experiments. Representative clones with reasonably uniform expression and expression levels were used for further experiments. A MDCKII transfectant expressing rabbit pIgAR was a kind gift of Walter Hunziker (University of Lausanne) (25) and was stably transfected with NH-tagged rab4 expression constructs (20) as described above. For experiments with filter-grown cells, the cells were seeded on 6- or 24-mm polycarbonate filters with 0.4-μm pore size (Corning Inc., Acton, MA) and cultured for 4 days. Media were changed every 2 days, and 5 mM sodium butyrate was added 16–18 h before experiments to enhance expression of cytomegalovirus-driven constructs.

Single Cycle Kinetics of ^{125}I-Tf—Cells were grown on 24-mm Transwell filters as described above, washed twice in MEM, 20 mM HEPES, pH 7.4, and 0.1% BSA (uptake medium) supplemented with 50 μM deferoxamine, and depleted from endogenous Tf for 45–60 min at 37 °C in the same medium. 2 μg/ml ^{125}I-Tf in uptake medium was bound at 4 °C at either the basolateral or apical side for 60–90 min. Next, the cells were washed three times with ice-cold PBS^{2+}, transferred to a 37 °C water bath, and chased for different periods of time. After the incubation, cells were washed for 10 min with ice-cold acid wash buffer (25 mM HOAc, pH 5, 150 mM NaCl, 50 μM deferoxamine, and 0.1% BSA) and PBS^{2+}, respectively, followed by a second cycle of washes of 5 min. Filters were cut from the holders and counted in the gamma counter, as was done for media and washes. Results represent a percentage of the total ^{125}I-Tf.

Distribution of TfR between the Apical and Basolateral Plasma Membrane—Cells were grown on 24-mm Transwell filters, washed twice in uptake medium supplemented with 50 μM deferoxamine, and depleted from endogenous TF for 45–60 min at 37 °C in the same medium. The cells were then incubated on ice for 2 h with 2 μg/ml ^{125}I-Tf in 0.5 ml of uptake medium at the basolateral or apical side. Nonspecific binding was assayed in the presence of 100-fold excess unlabeled Tf and was <10%. The cells were washed with PBS^{2+} containing 0.49 mM $MgCl_2$, 0.91 mM $CaCl_2$, and 0.1% BSA and subsequently washed with alternating acid and neutral washes as described above. Filters were excised, and ^{125}I was assayed in the acid washes and cells using a gamma counter.

Pulse-chase Experiments with ^{125}I-Tf after 16 °C Internalization—Cells were grown on 24-mm Transwell filters and depleted of endogenous Tf as described above. 1–3 μg/ml ^{125}I-Tf was internalized at the basolateral side in 1 ml of uptake medium (without deferoxamine) for 30 min at 16 °C. The cells were put on ice, washed twice with PBS^{2+}, washed once with MES buffer (20 mM 2-(*N*-morpholino)ethanesulfonic acid, pH 5, 130 mM NaCl, 2 mM $CaCl_2$, 0.1% BSA, and 50 μM deferoxamine), and washed once with PBS^{2+} (each wash was 10 min). The acid-neutral wash cycle was repeated once more, but for 5 min. Cells were then chased at 37 °C. After different periods of time, media were collected and saved for quantitation of ^{125}I-Tf. The cells were washed twice with ice-cold medium, and cell-associated ^{125}I-Tf was counted in the gamma counter. Results are expressed as a percentage of total ^{125}I-Tf in the media and on the filter. For some experiments 5 μg/ml brefeldin A (BFA) was added to the medium during the internalization and chase periods.

Secretion of gp80—Cells were grown on 24-mm Transwell filters as described above and depleted in 2 ml of MEM (Sigma) lacking methionine and cysteine (labeling medium) for 30 min at 37 °C. The cells were then incubated for 60 min at 37 °C in 0.5 ml of labeling medium containing 0.4 mCi/ml [^{35}S]methionine and [^{35}S]cysteine (Amersham Biosciences, Inc.). The cells were then washed on ice with MEM/0.1% BSA and chased at 37 °C. After 60 min, apical and basal media were harvested, and *N*-ethylmaleimide was added to 20 mM. gp80 was immunoprecipitated from the media as described previously (23) and boiled for 5 min in nonreducing sample buffer. Immunoprecipitates were resolved by SDS-PAGE on 12.5% minigels and analyzed by phosphorimaging.

Immunofluorescence Microscopy and Internalization of Fluorescence-labeled Tf—Cells grown on coverslips were subjected to immunofluorescence microscopy as described previously (26). Filter-grown cells were fixed for 5 min in 3% paraformaldehyde, 80 mM K-PIPES, pH 6.8, 5 mM EGTA, and 2 mM $MgCl_2$ and then fixed for 10 min in 3% paraformaldehyde and 100 mM NaB_4O_7, pH 11. The filters were washed three times in PBS and quenched in 1 mg/ml $NaBH_4$ and PBS for 15 min. This cycle was repeated once with a fresh $NaBH_4$ solution. Filters were cut from their inserts, permeabilized, and labeled with antibodies as described for cells grown on coverslips. Filters were mounted in 50% glycerol, 50% PBS, 0.1% NaN_3, and 100 mg/ml 1,4-diazabicyclo[2.2.2]octane (Fluka, Zwijndrecht, The Netherlands). For internalization experiments, cells were washed twice with MEM and 0.1% BSA and depleted from endogenous Tf as described above. Texas Red-Tf was internalized at 50 μg/ml in MEM and 0.1% BSA in cells grown on coverslips, whereas 25 μg/ml Alexa594-Tf was used for filter-grown cells. Steady-state uptake was done for 60 min at 37 °C. For pulse-chase experiments, cells were loaded with 25 μg/ml Alexa594-Tf from the basolateral surface at 16 °C. After 30 min, cells were cooled on ice, washed, and reincubated with fresh 37 °C medium. After different periods of time, the cells were cooled on ice, washed twice in MEM and 0.1% BSA, and treated for immunofluorescence microscopy as described above.

Immunogold Electron Microscopy—NHrab4/pIgAR double transfectants were grown on polycarbonate filters and fixed with 2% paraformaldehyde and 1% acrolein in 0.1 M sodium phosphate buffer, pH 7.4. After 2 h at room temperature, the cells were embedded in 10% gelatin and stored for cryoultramicrotomy as described previously (27). Ultrathin cryosections were cut perpendicular to polycarbonate filters and labeled with rabbit antibody against rab4 followed by 10 nm of protein A gold. The intracellular distribution of gold label was quantitated by counting gold particles associated with identifiable organelles on sections prepared from transfected and nontransfected control MDCK cells. To determine the labeling density per unit of membrane length, pictures were taken at ×15,000 magnification of rab4-labeled sections. A transparency displaying a squared lattice of lines that were 0.5 cm apart was put over the pictures and analyzed for intersections with the membranes of interest (28, 29). To quantitate the distribution of rab4 throughout the apical and basolateral cytoplasm, we divided the entire cytoplasm in three zones, above the nucleus, at the height of the nucleus, and below the nucleus. Gold particles in the three zones were counted and expressed per unit of membrane length.

Miscellaneous Methods—Human apo-Tf (Sigma) was saturated with Fe^{3+} as described previously (14), dialyzed against 20 mM HEPES, pH 7.8, and 150 mM NaCl at 4 °C, and stored at −80 °C. Iron-saturated Tf (500 μg) was incubated with five iodobeads (Pierce) and 1 mCi of Na^{125}I

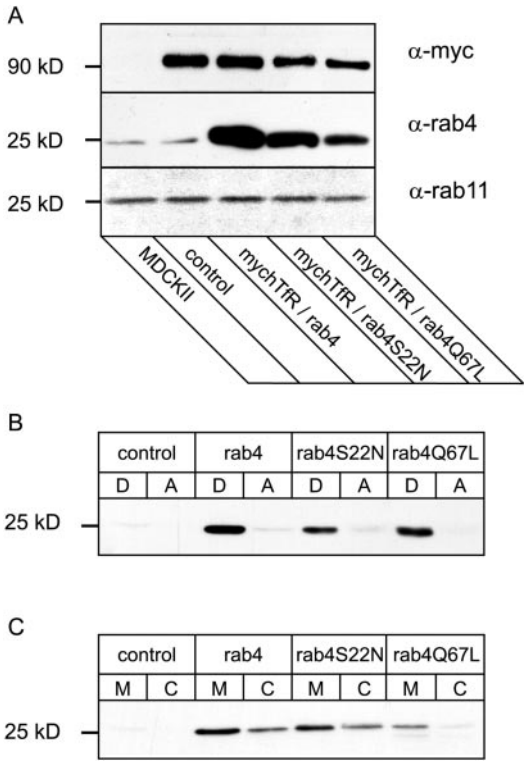

FIG. 1. **Characterization of transfected MDCK cells.** Nontransfected MDCKII cells and cells expressing myc-TfR (control), myc-TfR/rab4, myc-TfR/rab4S22N, and myc-TfR/rab4Q67L were lysed in 1% Triton X-100. Detergent lysates were analyzed by SDS-PAGE and Western blotting (*A*). Alternatively, cells were lysed in 1% Triton X-114, and detergent and aqueous phases were separated and subjected to SDS-PAGE and Western blotting (*B*). The distribution of ectopically expressed rab4 constructs was determined by subcellular fractionation as described under "Materials and Methods," and cytosol and membrane fractions were analyzed by SDS-PAGE and Western blot (*C*). Blots were probed with antibodies against rab4, c-myc, and rab11 (loading control).

(Amersham Biosciences, Inc.) in PBS. After 20 min at room temperature, the reaction mixture was applied to a PD-10 column (Amersham Biosciences, Inc.) to remove nonincorporated ^{125}I. ^{125}I-Tf was stored in 20 mM HEPES, pH 7.8, and 150 mM NaCl at −20 °C. Triton X-114 extractions were done as described previously (23). For subcellular fractionation, cells grown on a 6-cm dish were washed twice in MEM, scraped into 1 ml of MEM, and resuspended in 3 ml of HB (10 mM triethanolamine, pH 7.4, 10 mM acetic acid, 1 mM EDTA, and 0.25 M sucrose). The cells were then centrifuged at 1500 rpm for 10 min at 4 °C. The pellet was resuspended in 0.5 ml of HB, incubated for 15 min on ice, and broken by five passages through a 25-gauge needle. Postnuclear supernatant, membrane, and cytosol fractions were prepared as described and analyzed by Western blot (23). Detection was done with ECL reagent (Amersham Biosciences, Inc.).

RESULTS

Characterization of MDCK Transfectants—To investigate the role of rab4 in recycling from EEs in MDCK cells, we generated MDCK cell lines expressing rab4. Initially, we attempted to utilize the endogenous dog TfR as a read-out system to analyze the effects of rab4 overexpression. However, in our hands, this system could not routinely be used for this purpose. We therefore first generated MDCKII cells expressing human TfR with a myc epitope tag at the end of the cytoplasmic tail. After selection of positive clones, these cells were transfected with rab4, GTP hydrolysis mutant rab4Q67L, and dominant negative rab4S22N mutant that poorly binds guanine nucleotides. Human TfR was expressed to the same extent in the cell lines, as shown by the Western blot in Fig. 1*A*. Expression of the rab4 constructs was determined by Western blot using a rab4 antibody that binds the mutants with the same affinity as wild type rab4 (23). The rab4 constructs were expressed ~5–10 times above endogenous canine rab4, with ~2-fold lower expression in the rab4Q67L cell line. As a loading control for the amount of protein, we assayed endogenous rab11 in lysates of the transfectants (Fig. 1*A*).

Numerous studies have shown that rab proteins require prenylation of C-terminal Cys residues for membrane association. It is less clear, however, whether or not the GTP- and GDP-bound forms are efficient substrates for geranyl geranyltransferase type II. rab4 contains a canonical C-terminal C-G-C motif that is a typical substrate for geranyl geranyltransferase type II. To determine whether overexpressed rab4 proteins were prenylated, we performed Triton X-114 extractions in which prenylated protein partitions into the detergent phase, whereas nonprenylated protein is distributed in the aqueous phase (30). The two phases were resolved by SDS-PAGE and analyzed by Western blotting. As shown in Fig. 1*B*, more than 90% of overexpressed rab4 and the two mutants partitioned in the detergent phase, suggesting that the mutations did not affect the acquisition of geranyl-geranyl groups. To examine membrane association of the rab4 mutants, we performed subcellular fractionation. Cells were homogenized, and postnuclear supernatants were resolved in membrane and cytosol fractions. Membrane and cytosolic proteins were resolved by SDS-PAGE and analyzed by Western blot. As shown in Fig. 1*C*, rab4S22N and rab4Q67L were found to a similar extent in the membrane fraction as wild type rab4. Thus, rab4 and the two mutants were similarly prenylated and associated with membranes in the MDCKII transfectants.

Distribution of rab4—We next established the localization of rab4 in rab4-MDCKII cells by double label confocal microscopy. The cells were grown on coverslips and labeled with a polyclonal antibody against rab4. As shown in Fig. 2*A*, rab4 (*green*) localized to discrete cytoplasmic structures that were concentrated in the perinuclear area. These represented EEs because they also contained internalized Texas Red-Tf (*red*). We then compared the distribution of rab4S22N and rab4Q67L mutants with that of rab4. In cells expressing rab4S22N (Fig. 2*B*, *green*), most of the label was typically found in tubular structures close to the nucleus, whereas the scattered peripheral cytoplasmic staining seen with wild type rab4 had disappeared. In rab4Q67L transfectants (Fig. 2*C*, *green*), the GTPase-deficient mutant predominantly labeled ring-like structures around the nucleus. Consistent with these morphological alterations, we found significantly less colocalization of the mutants with endocytosed Texas Red-Tf in both cell lines.

Given the distinct labeling patterns of the two rab4 mutants, we next examined the distribution of EEA1 in rab4 transfectants. To facilitate detection of rab4 in double labeling experiments, we used MDCK cells transfected with epitope-tagged NHrab4, NHrab4S22N, or NHrab4Q67L. Antibodies against the rab5 effector protein EEA1 labeled distinct punctate structures (Fig. 2, *D–F*, *green*) throughout the cytoplasm in NHrab4 cells (Fig. 2*D*). These were similarly distributed and of the same size as those observed in nontransfected cells (data not shown) and partially colabeled with rab4 (*red*). In the cell lines expressing NHrab4S22N (Fig. 2*E*, *red*) and NHrab4Q67L (Fig. 2*F*, *red*), we found even less colocalization between EEA1 and the rab4 mutants. Taken together, these results suggested that rab4S22N and rab4Q67L induced distinct morphological alterations to regions of the early endosomal network in MDCK cells, which are relatively depleted of EEA1 and internalized Tf.

Endocytosis occurs from both the apical and basolateral domains of filter-grown MDCK cells, and indeed, rab5 is known to be involved in clathrin-mediated internalization from both sur-

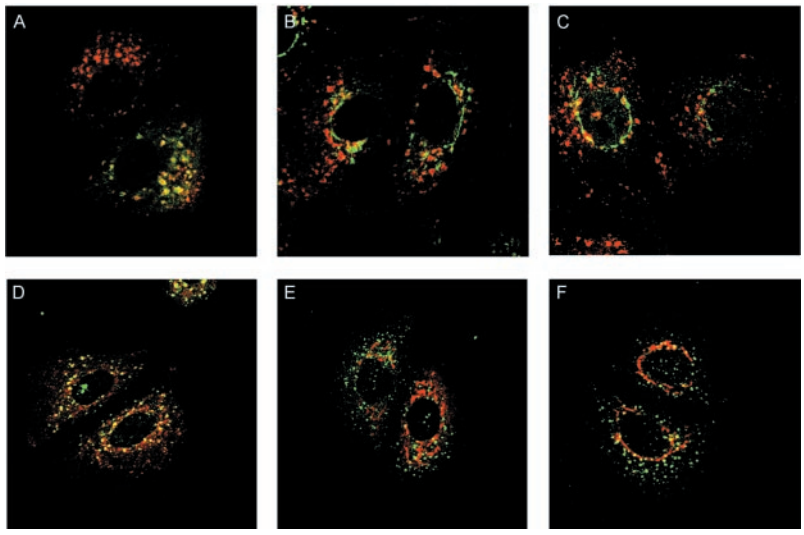

FIG. 2. **Morphological alterations of EEs in rab4S22N and rab4Q67L transfectants.** Cell lines expressing nontagged rab4 constructs were grown on coverslips and incubated for 30 min at 37 °C with 25 μg/ml Texas Red-Tf (*red, A–C*). The cells were fixed in 3% paraformaldehyde, labeled with a rabbit antibody against rab4, and stained with fluorescein isothiocyanate-labeled anti-rabbit antibody (*green*, *A–C*). Note the colocalization of rab4 and Texas Red-Tf (*A*) and the morphological changes caused by the mutants rab4S22N (*B*) and rab4Q67L (*C*). MDCKII cells expressing epitope-tagged rab4 (*red*, *D*), rab4S22N (*red*, *E*), or rab4Q67L (*red*, *F*) were labeled with a rabbit antibody against EEA1 and a monoclonal antibody against the epitope tag. The NH tag was stained with Cy3-labeled goat anti-mouse antibody (*D–F*), and EEA1 was detected with fluorescein isothiocyanate-labeled goat anti-rabbit antibody (*green*, *D–F*).

faces (11). Because rab4 and rab5 have opposing roles in EE membrane dynamics (31), we were interested to learn where rab4 localized in filter-grown MDCK cells. The rab4 MDCKII transfectants were fully polarized by growing them on Transwell filters. After fixation, the cells were labeled for rab4 (*green*) and the tight junction marker ZO-1 (*red*) and analyzed by double label confocal microscopy. In Fig. 3, consecutive 1.5-μm XY sections are shown from the filter (Fig. 3*A*) to the apical plasma membrane domain (Fig. 3*H*). Most of the rab4 staining was concentrated close to the nucleus at the height of ZO-1. In addition, we observed a weaker punctate labeling throughout the basolateral cytoplasm.

To further define the location of rab4 at the ultrastructural level, we used immunogold electron microscopy on ultrathin cryosections tangentially cut from filter-grown MDCKII cells stably transfected with NHrab4. More than 70% of gold particles were localized to vesicles and tubulovesicular structures in the apical and lateral cytoplasm, whereas very little label was present in the basal cytoplasm. The distribution of rab4 was quantitated from photographs taken at low magnification. The prints were then assembled to visualize the entire cell including the filter and apical plasma membrane. We divided the cytoplasm into three zones: one above, one below, and one at the height of the nucleus. In agreement with the confocal immunofluorescence data, we found most of rab4 above the nucleus (Table I). Because the basal cytoplasm of MDCK cells contains a less well-developed internal membrane network than the apical cytoplasm, we next quantitated the relative distribution of rab4 per unit of membrane length over tubulovesicular endosomes. Although we found most of the rab4 label associated with these structures in the upper third of the cell, Table I nevertheless shows that the density of rab4 labeling was similar in the three zones. Identical results were obtained when we used the NH epitope tag antibody to detect NHrab4.

Wild Type rab4 and rab4Q67L Relocate TfR to the Apical Cell Surface—In CHO transfectants expressing high levels of rab4, we previously found that TfR was redistributed from EEs to the plasma membrane (14). In polarized epithelia, a role for rab4 has not yet been determined. We therefore started to investigate the effect of rab4 on Tf recycling in filter-grown transfectants in single cycle experiments. After prebinding ^{125}I-Tf at the basolateral plasma membrane on ice, the cells were warmed at 37 °C for different periods of time, and cell-associated ^{125}I-Tf and ^{125}I-Tf present in basolateral and apical media were quantitated. As shown in Fig. 4*A*, we found similar ^{125}I-Tf

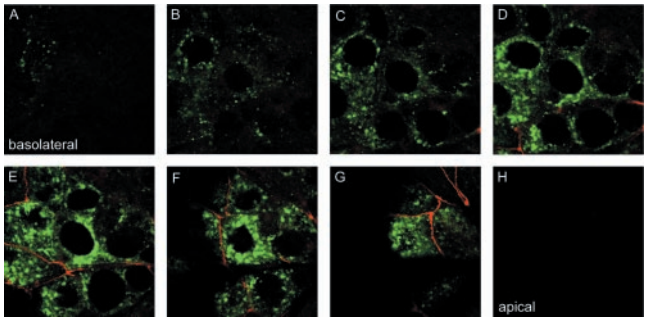

FIG. 3. **rab4 is concentrated at the level of the tight junction marker ZO-1.** myc-TfR/rab4 MDCKII transfectants were grown on 24-mm Transwell filters for 4 days. Cells were fixed with 3% paraformaldehyde and labeled with a rabbit antibody against rab4 and a monoclonal rat antibody against ZO-1. rab4 was detected with fluorescein isothiocyanate-labeled goat anti-rabbit antibody (*green*), and ZO-1 was detected with Texas Red-labeled goat anti-rat antibody (*red*). Merged images of consecutive optical sections are shown from the basolateral side to the apical side (*A–H*).

TABLE I
Distribution of rab4 in filter-grown MDCKII cells

Transfectants were grown on polycarbonate filters. After fixation, the cells were processed for immunoelectron microscopy as described. Sections were photographed at ×15,000 magnification, and prints from adjacent parts of the cell were assembled so that the entire cell was covered in the collage. The cytoplasm was then divided into three zones (above, below, and at the level of the nucleus). At least 300 gold particles were counted per cell in four rab4-transfected cells. Note that although ~5 times more gold particles were present on tubulovesicular endosomal membranes in the apical cytoplasm than in the basolateral cytoplasm, the density (expressed as % gold particles/ % membrane) of rab4 molecules per unit of membrane length is similar among the three regions.

	% gold	% membrane length	Density
Apical cytoplasm	73	65.7	1.1
Perinuclear cytoplasm	11.9	13.2	1.1
Basolateral cytoplasm	15.1	21.1	0.8

single cycle kinetics in the wild type and mutant rab4 cell lines. We also performed these experiments with ^{125}I-Tf that was prebound and internalized from the apical cell surface, and we obtained the same results (data not shown).

When moderate overexpression of rab4 has a limited effect on the kinetics of the TfR cycle, a single round of Tf uptake and recycling conceivably may lack the requisite sensitivity to discern the specific effects of rab4 mutants. Accordingly, we next

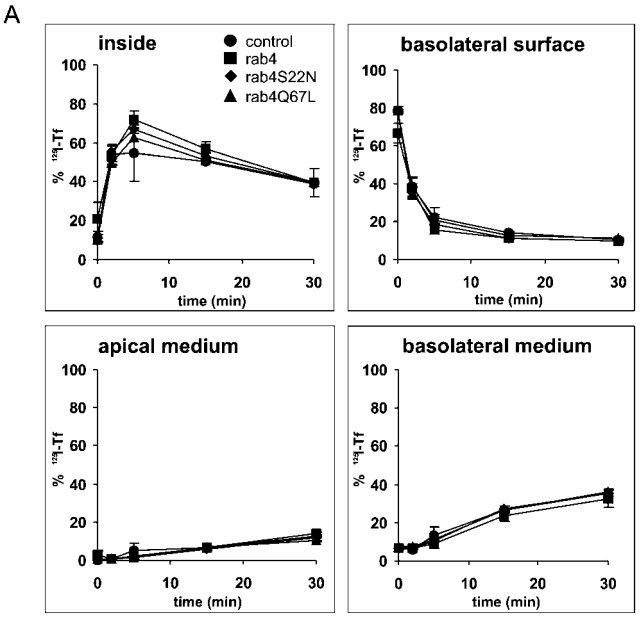

FIG. 4. **Wild type rab4 and rab4Q67L relocate TfR to the apical surface.** Transfectants were grown on 24-mm Transwell filters for 4 days. ^{125}I-Tf (2 μg/ml) was bound to the basolateral surface for 1.5 h on ice. The cells were washed and subsequently incubated with fresh medium at 37 °C for different periods of time. Apical and basal media were collected, and ^{125}I-Tf on the plasma membrane was removed with an acid wash. ^{125}I-Tf is expressed as a percentage of total cpm recovered from media and cells (*A*). Alternatively, ^{125}I-Tf was bound to the basolateral and apical surfaces on ice. After 1.5 h, the cells were washed, and membrane-associated ligand was removed with several acid washes. Filters and acid-washed fractions were counted (*B*). Data are the means ± S.D. of three experiments.

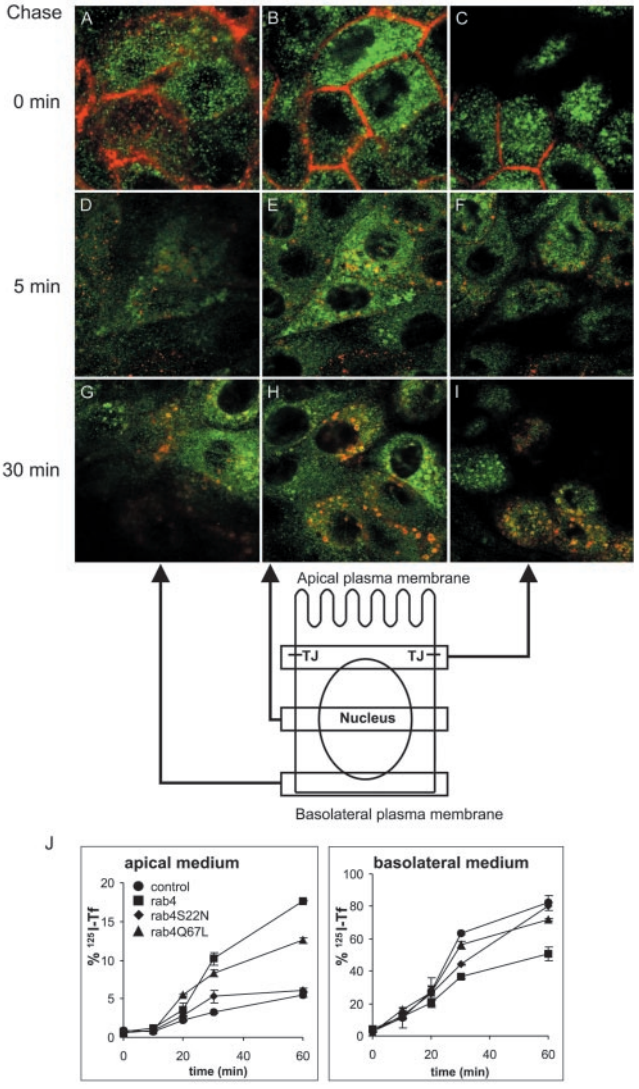

FIG. 5. **Wild type rab4 and rab4Q67L enhance apical transcytosis of ^{125}I-Tf.** MDCKII cells stably transfected with human TfR and rab4 were grown on 24-mm Transwell filters for 4 days. Alexa594-Tf was internalized for 30 min at 16 °C from the basolateral surface, and cells were then either fixed with 3% paraformaldehyde or surface-stripped at 4 °C (except for the cells that were not chased). Internalized Alexa594-Tf was subsequently chased for different periods of time at 37 °C. After fixation, filters were labeled with a polyclonal antibody against rab4. rab4 was detected with Alexa488 anti-rabbit antibody. Merged images of grouped optical sections are shown from the basolateral side to the apical side (*A*–*I*). MDCKII cells stably transfected with human TfR (control) or double-transfected with human TfR and rab4, rab4S22N, or rab4Q67L were grown on 24-mm Transwell filters for 4 days. Cells were loaded with ^{125}I-Tf at 16 °C for 30 min from the basolateral plasma side and incubated at 37 °C. Apical and basolateral media were collected at different time periods, and the amount of ^{125}I-Tf present is expressed as a percentage of the total. Data are the means ± S.D. of three experiments.

determined the steady-state distribution of TfR over the apical and basolateral plasma membranes. For this purpose, ^{125}I-Tf was bound on ice at the basolateral or apical plasma membrane. As shown in Fig. 4*B*, we found ~2 times more ^{125}I-Tf binding at the apical side of the rab4 transfectants as compared with the nontransfected control cells or cells expressing rab4S22N. In rab4Q67L-transfected cells, we also observed an increase in TfR at the apical plasma membrane, although this increase was somewhat smaller than that seen in the wild type rab4 transfectant. This might be caused by the slightly lower expression level of rab4Q67L (*cf.* Fig. 1). Thus, overexpression of rab4 and rab4Q67L caused a redistribution of TfR from the basolateral to the apical surface of the cell.

rab4 Enhances Apical Transcytosis of ^{125}I-Tf from Basolateral EEs—Because the cell surface binding assays showed an increase of ^{125}I-Tf binding at the apical cell surface in rab4 and rab4Q67L transfectants, we investigated whether delivery of basolaterally endocytosed Tf to the apical membrane was affected by rab4. To this end, we made use of previous observations that endocytosed ligands accumulate in sorting endosomes at 16 °C (32). Because it is not known whether this compartment is proximal to rab4-containing basolateral EEs, we first established the distribution of Alexa594-Tf endocytosed at 16 °C with respect to rab4 in filter-grown cells using confocal microscopy. As shown in the XY sections of Fig. 5, *A*–*C*, the internalized tracer (*red*) localized primarily to EEs in the proximity of the lateral plasma membrane and did not reach, to a significant extent, the rab4-containing EEs (*green*) at the level of ZO-1. When the cells were warmed to 37 °C,

Alexa594-Tf started to fill the rab4-containing compartments within 5 min, as evidenced by Fig. 5, *D–F*, whereas at 30 min, Tf reached the region containing the tight junction marker ZO-1 (Fig. 5, *G–I*). After 60 min, a large fraction of Alexa594-Tf was chased out of the cells (data not shown). Having shown that the 16 °C compartment was proximal to rab4-containing endosomes, we next internalized ^{125}I-Tf for 30 min at 16 °C from the basal surface. After removal of cell surface-bound ^{125}I-Tf, cells were chased for different periods of time at 37 °C. As shown in Fig. 5*J*, control cells transfected with TfR recycled up to 5% of basolaterally endocytosed ^{125}I-Tf to the apical side, whereas in rab4 and rab4Q67L transfectants, 2–3 times more ^{125}I-Tf was transcytosed after 60 min into the apical medium. In contrast, in MDCK cells expressing rab4S22N, we found the same extent of apical transcytosis as in the control cells. Similar results were obtained when ^{125}I-Tf was internalized at 16 °C from the apical plasma membrane (data not shown). Thus, in agreement with the binding experiments, ectopically expressed rab4 and rab4Q67L, but not dominant negative rab4S22N, perturbed polarized transport of ^{125}I-Tf.

We also evaluated the transfer of dIgA from basolateral EEs to the apical cell surface in NHrab4/pIgAR transfectants. dIgA (50 μg/ml) was internalized for 30 min at 16 °C, and cells were washed twice to remove extracellular ligand. After different chase periods at 37 °C, cells were fixed and processed for confocal microscopy. At the end of the pulse, dIgA was accumulated in early endocytic structures with a predominantly lateral localization that contained little, if any, rab4. Upon chase at 37 °C, IgA left the lateral endosomes and moved to NHrab4-containing structures in the juxtanuclear region (Fig. 6*H*). Upon longer chase times, IgA exited these compartments and accumulated in subapical organelles that did not label for NHrab4. This was confirmed in immunofluorescence experiments, where the cells were labeled with antibodies against pIgAR and NHrab4. Most of the pIgAR was concentrated in this subapical compartment that excluded NHrab4 (data not shown). Thus, IgA, in contrast to Tf, transiently resided in rab4-containing endosomes, whereas Tf was seen at most chase times to colocalize with NHrab4, even in the apical cytoplasm.

Brefeldin A and rab4 Regulate Tf Transport from EEs—Previous ultrastuctural experiments showed that internalized TfR is localized to the CE that is coated with clathrin lattices and decorated with γ-adaptin-coated buds (5). In the presence of BFA, these coats are not formed, and polarized targeting of TfR in MDCK cells is lost (5). In fibroblasts, BFA was reported to cause a small decrease in the rate of TfR recycling (33). Because rab4 also reduced the polarity of TfR sorting, we next investigated whether BFA and rab4 had synergistic effects on TfR recycling. When nontransfected MDCK cells were treated with BFA, we found that 30% of basolaterally endocytosed ^{125}I-Tf was transcytosed into to the apical medium after 2 h. In cells transfected with rab4 or rab4Q67L, there was no additional effect of BFA on apical transcytosis of ^{125}I-Tf (Fig. 7), whereas we found a slight decrease in basolateral recycling of ^{125}I-Tf, probably due to retarded transport causing intracellular accumulation of ^{125}I-Tf. These results suggested that rab4 and BFA may act in the same, but not parallel, TfR transport pathways.

Apical Secretion of Glycoprotein 80 Is Not Altered in rab4 Transfectants—To investigate whether enhanced recycling of ^{125}I-Tf into the apical medium in cells transfected with rab4 and rab4Q67L was due to pleiotropic effects of rab4 expression, we next investigated the secretion of gp80. This 80-kDa sulfated protein is constitutively secreted in a polarized fashion into the apical medium of filter-grown MDCK cells (34). Transfectants were metabolically labeled for 60 min with ^{35}S TranS

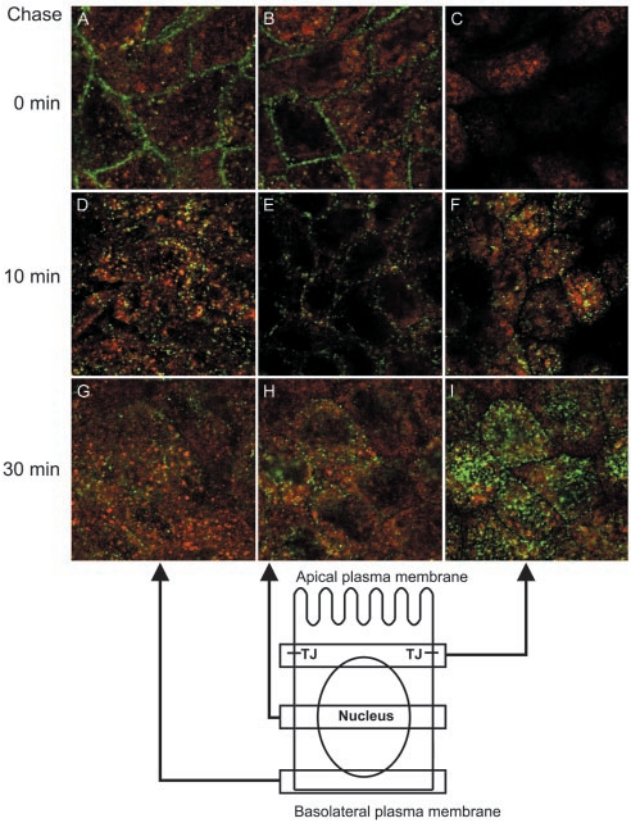

FIG. 6. **Transcytosis of dIgA in polarized NHrab4 transfectants.** MDCKII cells stably transfected with NHrab4 and pIgAR were grown on 24-mm Transwell filters for 4 days. 50 μg/ml dIgA was internalized basolaterally for 1 h at 16 °C. The cells were washed on ice and reincubated with fresh 37 °C medium for 0, 10, or 30 min. Cells were fixed as described under "Materials and Methods" for the Tf pulse-chase experiments and labeled with a monoclonal antibody against the NH tag (*red*) and a rabbit polyclonal antibody against IgA (*green*). The NH tag was detected with Cy3 anti-mouse antibody, and dIgA was detected with Alexa488 anti-rabbit antibody. Merged images of different optical sections are shown from the basolateral side to the apical side (*A–I*).

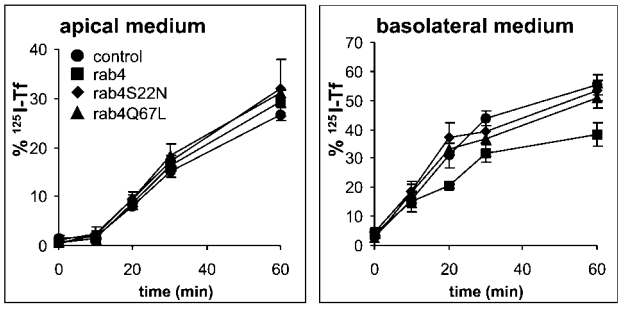

FIG. 7. **BFA enhances apical transcytosis of ^{125}I-Tf independent of rab4.** Transfectants were grown on 24-mm Transwell filters for 4 days. ^{125}I-Tf (2 μg/ml) was internalized at 16 °C from the basolateral plasma membrane in the presence of 5 μg/ml BFA. Cells were washed after 30 min and and reincubated at 37 °C with fresh medium containing 5 μg/ml BFA. Apical and basolateral media were collected after different periods of chase time. The amount of ^{125}I-Tf is expressed as a percentage of the total cpm recovered from washes, media, and cell fractions. Data are the means ± S.D. of three experiments.

label and chased for 60 min. At the end of the chase time, we immunoprecipitated gp80 from the apical and basolateral media. Immunoprecipitates were resolved by SDS-PAGE under nonreducing conditions and analyzed by phosphorimaging. As shown in Fig. 8, most of the gp80 molecules were apically secreted in control cells. When we quantitated the extent and

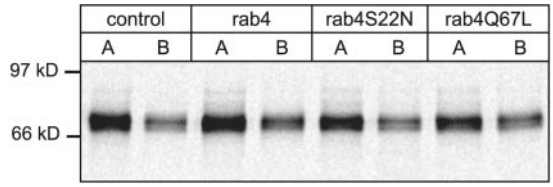

FIG. 8. **Polarized secretion of gp80 is not affected by rab4.** MDCK transfectants were grown on 24-mm Transwell filters for 4 days. Cells were depleted for 30 min in methionine- and cysteine-deficient medium, labeled with ^{35}S TranS for 60 min at 37 °C, and chased for 60 min at 37 °C. Apical and basolateral media were collected, from which gp80 was immunoprecipitated with a polyclonal antibody. Immunoprecipitates were resolved by SDS-PAGE under nonreducing conditions and analyzed by phosphorimaging.

polarity of gp80 secretion in the rab4 transfectants, we found that ~75% of gp80 was apically secreted and that neither wild type rab4 nor the two mutants affected biosynthesis, maturation, and polarized targeting of gp80. Given these results, it is unlikely that the increased apical transcytosis of ^{125}I-Tf we observed in rab4 and rab4Q67L transfectants was caused by general effects of rab4 overexpression on membrane transport.

DISCUSSION

Membrane transport through the endocytic pathway has been extensively investigated in the MDCK cell line, a model system for polarized epithelia. Although the basic outline of the intracellular transport pathways connecting the basolateral and apical plasma membranes has been defined, it is clear that much remains to be learned about the compartmental boundaries, the proteins that endow EEs with their specific properties, and the molecules regulating transport between these compartments. We have been focusing on rab4, a small GTPase that is involved in membrane recycling from EEs in fibroblasts. Initially, we found that rab4 is expressed in MDCK cells; however, its function in the endocytic pathway of polarized epithelia has not yet been addressed.

Here we generated an MDCK cell line ectopically expressing TfR to facilitate the analysis of Tf endocytosis, recycling to the basolateral plasma membrane, and transcytosis to the apical cell surface. This cell line was subsequently double-transfected with rab4 cDNA or an active mutant deficient in GTP hydrolysis and an inhibitory mutant that poorly binds GDP to investigate the role of the small GTPase in MDCK cells. Our results show that rab4 is localized on early endocytic compartments or transport vesicles that are positioned distally to basolateral EEs and concentrated in the apical cytoplasm and suggest that rab4 regulates transport through or from this compartment. These conclusions are based on the following observations. First, all intracellular structures that contain rab4 are accessible to endocytosed Tf. Second, rab4 colocalized to a limited extent with EEA1, a marker of basolateral EEs in MDCK cells (12). Third, pulse-chase experiments with fluorescence-labeled Tf revealed that the rab4-containing endosomes were only reached during the chase period at 37 °C, whereas EEA1-labeled endosomes were already filled by the tracer during the pulse at 16 °C. Fourth, expression of rab4 caused missorting of TfR and enhanced transcytosis of ^{125}I-Tf into the apical medium of filter-grown MDCK cells.

Understanding the complexity of polarized endosomal compartments in epithelial cells requires the availability of a set well-defined marker proteins. Transport of membrane-bound ligands from the basolateral plasma membrane to the apical membrane appears to involve at least three endosomal compartments in MDCK cells. Receptors internalized from the basolateral cell surface first reach basolaterally localized EEs, which contain IgA and Tf. The next compartment these ligands enter is a 60-nm-diameter tubularized endosome that contains IgA and Tf at the same concentrations but is relatively depleted of proteins destined for degradation. Endocytosed IgA and Tf from the apical or basolateral surface meet in this compartment, hence, its name is the common endosomal compartment. The CE appears to be positioned along microtubules and is oriented toward the apical cytoplasm (35). The third compartment, called the ARE, consists of 100–150-nm, cup-shaped vesicles distributed immediately below the apical surface. This compartment is enriched in basolaterally endocytosed IgA and depleted of TfR with respect to the CE. Ultrastuctural studies in MDCK cells (5) and cell fractionation of rat liver suggested that the ARE and tubular CE probably represent a single compartment that might be divided into different domains (5, 36). This was largely based on the observation that whenever TfR and IgA colocalized, their relative concentrations appeared to be the same. Recent fluorescence ratio imaging studies in MDCK cells, however, show that the lumenal pH of the ARE is significantly less acidic than that of the CE (6), which is difficult to reconcile with a physical continuity between CE and the ARE and argues for the case of distinct biochemical entities (37). The observations that rab4 colocalized to a limited extent with EEA1 and not with internalized Tf at 16 °C show that basolateral EEs represent only a limited subset of rab4-positive compartments. The density of the membrane-associated rab4 signal increased from the basolateral cytoplasm toward the apical cytoplasm just below the tight junction marker ZO-1. Internalized dIgA did not colocalize with rab4 after longer chase periods, and most of pIgAR is in structures that are closer to the apical plasma membrane than rab4, which strongly suggest that rab4 is associated with the tubular CE domain. Our results are consistent with subcellular fractionation experiments of MDCK cells, where the small G protein was found in purified recycling endosomes (9).

What might be the function of rab4 on the CE? Important clues with respect to this question are provided by the effect of BFA on basolateral targeting of Tf. BFA causes significant changes in the morphology of endosomes in MDCK cells, although the sequential arrangement of EEs, the CE, and the ARE as well as their biochemical identity reportedly remains intact (38) in the presence of BFA. BFA and, to a somewhat lesser extent, transfected rab4 abrogate polarized recycling of TfR to the basolateral plasma membrane in MDCK cells, and significantly more TfR is transported to the apical plasma membrane, suggesting an effect on polarized sorting (5, 38). In agreement with this, BFA causes dispersal of γ-adaptin-containing clathrin lattices from the CE in filter-grown MDCK cells (5), whereas in CHO (21) and A431 cells (39), BFA induces extensive tubulation of endosomal membranes enriched in Tf and rab4-containing domains. We found that rab4 is primarily localized to the CE, and because the effect of BFA on polarized sorting appears to be at the level of this organelle (38), these independent observations suggested that rab4 and BFA may act in the same transport step with respect to apical Tf transcytosis in polarized MDCK cells. To test this hypothesis, we examined the effect of BFA on Tf sorting in rab4-transfected cell lines. If rab4 and BFA regulated distinct routes of Tf transport through endosomes, a synergistic effect of rab4 on BFA-mediated missorting of Tf would be anticipated. In contrast, if rab4 and BFA acted in the same transport pathway, such synergism would not be expected. This is precisely what we found and is consistent with recent data documenting a role of rab4 in the formation of TfR-containing vesicles (17). Nevertheless, because BFA affects the assembly of multiple coats on different intracellular organelles, and because the association of the AP-1 subunit, γ-adaptin, with distinct compartments of

the transcytotic pathway is inhibited by BFA (39), it is clear that alternative explanations cannot be excluded. Formally, a sequential arrangement of activities of rab4 and of a BFA-sensitive target in the transcytotic pathway taken by basolaterally internalized Tf would also be consistent with the absence of synergism between rab4 and BFA to enhance Tf transcytosis. However, the latter possibility is less likely, given the predominant localization of rab4 to the CE and the observation of Dunn and co-workers (38) that the effect of BFA on polarized sorting in the transcytotic pathway is primarily at the level of the CE. Finally, the notion that Tf recycling occurs by bulk flow (40) and that BFA has little, if any, effect on TfR recycling (41–43) argues against the possibility that enhanced apical transport of Tf is caused by inhibited basolateral recycling at the level of the basolateral EE. How rab4 and BFA regulate transcytosis from the CE is not known. However, rab4 effectors may cross-talk with ARF1-dependent pathways. Rabaptin variants have been identified that interact with rab4 (and rab5) (22, 44). Interestingly, rabaptins also bind to γ-adaptin and the ARF1 effector GGA2 (45, 46) and thereby might regulate ARF1-dependent budding events from endosomes. The functional significance of the link between rab4, its effector proteins, and ARF1-interacting proteins in protein sorting and vesicle budding, however, will have to await further experimentation.

A few rab proteins have been localized to early endocytic compartments in epithelial cells. Ubiquitously expressed rab5 is associated with apical EEs and basolateral Ees, and its overexpression enhances delivery of endocytosed material from both plasma membrane domains to EEs (11). The function of three other rab GTPases (rab11, its epithelial homolog rab25, and epithelial-specific rab17) has recently been evaluated. rab11 and rab25 associate with the ARE (38, 47, 48) and are thought to regulate the delivery of transcytotic IgA cargo molecules to the apical plasma membrane while having little or no effect on basolateral Tf recycling. The situation with rab17 is less clear; it is also localized to the ARE of MDCK and Eph4 cells, however, its overexpression had contradictory effects on the transcytotic pathway (49, 50). These data suggest that rab11/rab25 and rab17 appear to be localized more apically than rab4 in the pathways connecting the basolateral and apical plasma membrane domains. At least with respect to rab4 and rab11, this situation is reminiscent of their functional domain organization in nonepithelial cells (39), in which rab11 regulates transport distal to rab4. Possibly rab4, rab11/rab25, and rab17, through interactions with bifunctional effectors, form overlapping subdomains of the endosomal system and regulate transfer of ligands between these subdomains to various destinations in MDCK cells, as has been proposed for rab5, rab4, and rab11 in nonpolarized cells (39). This hypothesis is in agreement with the observation of an interconnected endocytic compartment in which polarized sorting to apical and basolateral domains occurs in epithelial cells (4, 38). A first test of this hypothesis will require a critical evaluation of the comparative localization of these rab proteins in the same cell.

Acknowledgments—Walter Hunziker, Karl Matter, Michael Clague, Claudia Koch-Brandt, Jean-Pierre Vaerman, and Jim Casanova are acknowledged for generously sharing reagents. We thank members of our laboratory and the Department of Cell Biology for critical discussion and helpful suggestions.

REFERENCES

1. Mellman, I. (1996) *Annu. Rev. Cell Dev. Biol.* **12,** 575–626
2. Bomsel, M., Prydz, K., Parton, R., Gruenberg, J., and Simons, K. (1989) *J. Cell Biol.* **109,** 3243–3258
3. Barroso, M., and Sztul, E. S. (1994) *J. Cell Biol.* **124,** 83–100
4. Odorizzi, G., Pearse, A., Domingo, D., Trowbridge, I. S., and Hopkins, C. R. (1996) *J. Cell Biol.* **135,** 139–152
5. Futter, C. E., Gibson, A., Allchin, E. H., Maxwell, S., Ruddock, L. J., Odorizzi, G., Domingo, D., Trowbridge, I. S., and Hopkins, C. R. (1998) *J. Cell Biol.* **141,** 611–624
6. Wang, E., Brown, P. S., Aroeti, B., Chapin, S. J., Mostov, K. E., and Dunn, K. W. (2000) *Traffic* **1,** 480–493
7. Apodaca, G., Katz, L. A., and Mostov, K. E. (1994) *J. Cell Biol.* **125,** 67–77
8. Apodaca, G. (2001) *Traffic* **2,** 149–159
9. Gagescu, R., Demaurex, N., Parton, R. G., Hunziker, W., Huber, L. A., and Gruenberg, J. (2000) *Mol. Biol. Cell* **11,** 2775–2791
10. Sheff, D. R., Daro, E. A., Hull, M., and Mellman, I. (1999) *J. Cell Biol.* **145,** 123–139
11. Bucci, C., Wandinger-Ness, A., Lütcke, A., Chiarello, M., Bruni, C. B., and Zerial, M. (1994) *Proc. Natl. Acad. Sci. U. S. A.* **91,** 5061–5065
12. Wilson, J. M., de Hoop, M., Zorzi, N., Toh, B. H., Dotti, C. G., and Parton, R. G. (2000) *Mol. Biol. Cell* **11,** 2657–2671
13. Tuma, P. L., Nyasae, L. K., Backer, J. M., and Hubbard, A. L. (2001) *J. Cell Biol.* **154,** 1197–1208
14. van der Sluijs, P., Hull, M., Webster, P., Goud, B., and Mellman, I. (1992) *Cell* **70,** 729–740
15. Bottger, G., Nagelkerken, B., and van der Sluijs, P. (1996) *J. Biol. Chem.* **271,** 29191–29197
16. de Wit, H., Lichtenstein, Y., Geuze, H., Kelly, R. B., van der Sluijs, P., and Klumperman, J. (1999) *Mol. Biol. Cell* **10,** 4163–4176
17. de Wit, H., Lichtenstein, Y., Kelly, R. B., Geuze, H. J., Klumperman, J., and van der Sluijs, P. (2001) *Mol. Biol. Cell* **12,** 3703–3715
18. Roberts, M., Barry, S., Woods, A., van der Sluijs, P., and Norman, J. (2001) *Curr. Biol.* **11,** 1392–1402
19. Evan, G. I., Lewis, G. K., Ramsay, G., and Bishop, J. M. (1985) *Mol. Cell. Biol.* **5,** 3610–3616
20. Nagelkerken, B., Mohrmann, K., Gerez, L., van Raak, M., Leijendekker, R. L., and van der Sluijs, P. (1997) *Electrophoresis* **18,** 2694–2698
21. Daro, E., van der Sluijs, P., Galli, T., and Mellman, I. (1996) *Proc. Natl. Acad. Sci. U. S. A.* **93,** 9559–9564
22. Nagelkerken, B., van Anken, E., van Raak, M., Gerez, L., Mohrmann, K., van Uden, N., Holthuizen, J., Pelkmans, L., and van der Sluijs, P. (2000) *Biochem. J.* **346,** 593–601
23. Gerez, L., Mohrmann, K., van Raak, M., Jongeneelen, M., Zhou, X. Z., Lu, K. P., and van der Sluijs, P. (2000) *Mol. Biol. Cell* **11,** 2201–2211
24. Podbilewicz, B., and Mellman, I. (1990) *EMBO J.* **9,** 3477–3487
25. Hunziker, W., Whitney, J. A., and Mellman, I. (1991) *Cell* **67,** 617–627
26. Sprong, H., Kruithof, B., Leijendekker, R., Slot, J. W., van Meer, G., and van der Sluijs, P. (1998) *J. Biol. Chem.* **273,** 25880–25888
27. Peters, P. J., Neefjes, J. J., Oorschot, V., Ploegh, H. L., and Geuze, H. J. (1991) *Nature* **349,** 669–676
28. Weibel, E. R., Staubli, W., Gnagi, H. R., and Hess, F. A. (1969) *J. Cell Biol.* **42,** 68–91
29. Staubli, W., Hess, R., and Weibel, E. R. (1969) *J. Cell Biol.* **222,** 92–112
30. van der Sluijs, P., Hull, M., Huber, L. A., Male, P., Goud, B., and Mellman, I. (1992) *EMBO J.* **11,** 4379–4389
31. Chavrier, P., van der Sluijs, P., Mishal, Z., Nagelkerken, B., and Gorvel, J. P. (1997) *Cytometry* **29,** 41–49
32. Clift-O'Grady, L., Desnos, C., Lichtenstein, Y., Faundez, V., Horng, J. T., and Kelly, R. B. (1998) *Methods* **16,** 150–159
33. Schonhorn, J., and Wessling-Resnick, M. (1994) *Mol. Cell. Biochem.* **135,** 159–169
34. Urban, J., Parczyk, K., Leutz, A., Kayne, M., and Kondor-Koch, C. (1987) *J. Cell Biol.* **105,** 2735–2743
35. Gibson, A., Futter, C. E., Maxwell, S., Allchin, E. H., Shipman, M., Kraehenbuhl, J. P., Dimingo, D., Odorizzi, G., Trowbridge, I. S., and Hopkins, C. R. (1998) *J. Cell Biol.* **143,** 81–94
36. Verges, M., Havel, R. J., and Mostov, K. E. (1999) *Proc. Natl. Acad. Sci. U. S. A.* **96,** 10146–10151
37. Brown, P. S., Wang, E., Aroeti, B., Chapin, S. J., Mostov, K. E., and Dunn, K. W. (2000) *Traffic* **1,** 120–140
38. Wang, E., Pennington, J. G., Goldenring, J. R., Hunziker, W., and Dunn, K. W. (2001) *J. Cell Sci.* **114,** 3309–3321
39. Sönnichsen, B., De Renzis, S., Nielsen, E., Rietdorf, J., and Zerial, M. (2000) *J. Cell Biol.* **149,** 901–913
40. Mayor, S., Presley, J., and Maxfield, F. (1993) *J. Cell Biol.* **121,** 1257–1270
41. Lippincott-Schwartz, J., Yuan, L., Tipper, C., Amherdt, M., Orci, L., and Klausner, R. D. (1991) *Cell* **67,** 601–616
42. Damke, H., Klumperman, J., von Figura, K., and Braulke, T. (1991) *J. Biol. Chem.* **266,** 24829–24833
43. Martys, J. L., Shevell, T., and McGraw, T. E. (1995) *J. Biol. Chem.* **270,** 25976–25984
44. Vitale, G., Rybin, V., Christoforidis, S., Thornqvist, P. O., McCaffrey, M., Stenmark, H., and Zerial, M. (1998) *EMBO J.* **17,** 1941–1951
45. Boman, A. L., Zhang, C. J., Zhu, X., and Kahn, R. A. (2000) *Mol. Biol. Cell* **11,** 1241–1255
46. Hirst, J., Lui, W. W. Y., Bright, N. A., Totty, N., Seaman, M. N. J., and Robinson, M. S. (2000) *J. Cell Biol.* **149,** 67–69
47. Casanova, J. E., Wang, X., Kumar, R., Bhartur, S. G., Navarre, J., Woodrum, J. E., Altschuler, Y., Ray, G. S., and Goldenring, J. R. (1999) *Mol. Biol. Cell* **10,** 47–61
48. Wang, X., Kumar, R., Navarre, J., Casanova, J. E., and Goldenring, J. R. (2000) *J. Biol. Chem.* **275,** 29138–29146
49. Zacchi, P., Stenmark, H., Parton, R. G., Orioli, D., Lim, F., Giner, A., Zerial, M., and Murphy, C. (1998) *J. Cell Biol.* **140,** 1039–1053
50. Hunziker, W., and Peters, P. J. (1998) *J. Biol. Chem.* **273,** 15734–15741

rab4 Regulates Transport to the Apical Plasma Membrane in Madin-Darby Canine Kidney Cells

Karin Mohrmann, Richtje Leijendekker, Lisya Gerez and Peter van der Sluijs

J. Biol. Chem. 2002, 277:10474-10481.
doi: 10.1074/jbc.M111237200 originally published online January 14, 2002
